

Studies on equatorial waves over the Indian zone

M. N. Sasi¹, Geetha Ramkumar¹ and B. V. Krishna Murthy^{2,*}

¹Space Physics Laboratory, Vikram Sarabhai Space Centre, Thiruvananthapuram 695 022, India

²B1, Ceebros, 47/20, 3rd Main Road, Gandhi Nagar, Adyar, Chennai 600 020, India

As part of the Indian Middle Atmosphere Programme, three scientific campaigns were conducted to study equatorial waves in 1984, 1986 and 1988 from Trivandrum, SHAR and Balasore involving RH 200 rockets and balloonsondes for measurement of horizontal wind components. With the installation of MST radar and Rayleigh lidar at Gadanki, temperature could be determined in the middle atmosphere, enabling estimation of vertical flux of zonal momentum of the equatorial waves, which is a crucial parameter to understand the role of the equatorial waves in the generation of quasi biennial oscillation and semi annual oscillation. Making use of these facilities, three more campaigns were conducted to delineate the equatorial wave characteristics, including the wave momentum flux. The results of each of these campaigns have already been published. Here the results from all the six campaigns are reviewed, consolidated and examined in the light of the current global scenario of equatorial wave studies.

Keywords: Equatorial waves, Kelvin waves, momentum flux, momentum flux divergence, semi-annual oscillation.

LARGE-scale equatorially confined wave motions have been observed to propagate vertically and zonally through the middle atmosphere. The periods of these waves are in the range of ~3 to 25 days. These are of planetary scale in the zonal direction, but are trapped latitudinally within $\pm 15^\circ$ of the equator. These waves are generally referred to as equatorial waves. Of these, Kelvin and Rossby Gravity (RG) waves are prominent. Kelvin waves propagate in the eastward direction, while RG waves propagate in the westward direction. The wave perturbations manifest themselves in wind and temperature. Among the horizontal wind components, Kelvin wave disturbances appear only in the zonal wind, whereas RG wave disturbances appear both in zonal and meridional components, except at the equator where the zonal component, perturbation is zero.

The Kelvin and RG waves are generally thought to be forced by geographically confined time variations in the large-scale cumulus convective heating in the equatorial troposphere. Randomly distributed sources excite the longest zonal scale Kelvin waves most efficiently and that the

preferred vertical wavelength of the excited waves is about twice the vertical scale of the heat source¹. It is known that a localized tropical heat source asymmetric about the equator with a five-day period can generate an RG wave response that is dominated by wave number 4 in the lower stratosphere^{2,3}. The relatively slow-moving Kelvin and RG wave modes observed in the upper troposphere and lower stratosphere are effectively damped out by thermal dissipation (radiative damping) in the upper stratosphere. However, fast-moving Kelvin waves can penetrate into the mesosphere⁴.

Decrease in density with altitude results in growth of wave amplitudes to keep the associated kinetic energy constant, as the waves propagate vertically in the absence of any damping. The main damping processes for the equatorial waves are radiative damping due to Newtonian cooling and critical-level damping. In critical-level damping, waves lose their momentum and energy in a vertically sheared mean flow close to a level where the mean flow velocity is about the same as the wave phase velocity. Of the two, radiative damping is the dominating damping process⁵. When wave damping takes place, the waves lose their energy and momentum to the mean flow, thus accelerating it. This process is called the wave mean flow interaction and is the main process for the generation of equatorial stratospheric quasi biennial oscillation (QBO) and semi annual oscillation (SAO) in the equatorial stratosphere and mesosphere⁶. In fact, much of the early work on equatorial waves was spurred by their role in the generation of the QBO and SAO, which are the dominant long-period oscillations in the equatorial middle atmosphere. Besides the planetary-scale equatorial waves, gravity waves also play a crucial role in providing input to the generation of QBO and SAO through wave mean flow interaction. A key parameter in the theoretical understanding of the wave mean flow interaction process in the generation of QBO and SAO is the vertical flux of the horizontal momentum of the causative waves.

There have been a number of investigations on the delineation of equatorial wave characteristics and a few on the wave momentum fluxes^{7,8}. But almost all these were confined to data over Pacific and Atlantic zones. At least prior to 1980s this was the scenario. With the launching of the Indian Middle Atmosphere Programme in the 1980s, study of the middle atmospheric dynamics received a great fillip in India. This was facilitated by the availability of sounding rockets like RH 200 and high-altitude balloons for the studies on

*For correspondence. (e-mail: bvkurthy2@rediffmail.com)

middle atmosphere. For the first time, a concerted scientific campaign was conducted during May–June 1984 using RH 200 rockets for wind measurement in the altitude range 25 to 60 km and high-altitude balloonsondes for wind and temperature measurement in the altitude range 0 to ~28 km from three locations, namely Trivandrum (8.6°N, 77°E), SHAR (13.7°N, 80.2°E) and Balasore (21.5°N, 86.9°E). This was followed by two more campaigns using RH 200 rockets and balloonsondes in January–February 1986 from SHAR and in June–July 1988 from Trivandrum. In the 1988 campaign, balloonsondes were also launched from Minicoy (8.3°N, 73°E) and Port Blair (11.7°N, 92.7°E) to provide longitudinal coverage.

As stated earlier, the vertical flux of horizontal momentum of the equatorial waves is a crucial parameter for understanding and assessing the role of equatorial waves in the generation of QBO and SAO. While the campaigns conducted in 1984, 1986 and 1988 provided valuable data on winds for the first time in the Indian zone to delineate the equatorial wave characteristics, information on wave momentum fluxes could not be obtained from these campaigns. This was because of non-availability of instruments to measure the vertical component of wind and/or the temperature with the required degree of temporal and spatial resolutions. This vertical component of wind and/or temperature is essential for the estimation of wave momentum fluxes besides the horizontal components of the wind. With the installation of MST radar and Rayleigh lidar in the early and late 1990s respectively, at Gadanki (13.5°N, 79.2°E), vertical wind and temperature became accessible parameters for measurement. In 1995, with MST radar alone for the measurement of all the three components of wind in the altitude range ~4 to 25 km and in 1999 with MST radar and lidar for measurement of the three wind components in the altitude range ~4 to 25 km and temperature in the altitude range ~4 to 75 km, two experiments were conducted to obtain information on momentum fluxes^{9,10}. In 2000, a comprehensive experimental campaign was conducted using RH 200 rockets and balloonsondes from SHAR and MST radar and lidar at Gadanki, to delineate the equatorial wave modes and to estimate the wave momentum fluxes. This is perhaps the most comprehensive experimental campaign conducted ever for the study of equatorial waves, providing a unique dataset of temperature and winds from troposphere to mesosphere at nearly the same locations over a period of 45 days¹¹. The locations of

SHAR and Gadanki are separated by ~70 km and in view of the scales involved in equatorial waves, this separation is inconsequential for delineating the equatorial wave characteristics.

Here we review, consolidate and sum up the results obtained in all the experiments/campaigns mentioned above and present them in the overall perspective of current global scenario of equatorial waves.

Details of equatorial wave campaigns

The schedule and details of the experiments conducted in all the campaigns are given in Table 1. A brief description of the experiments is given below. Further details are available in the references given for each campaign.

(i) RH 200 rocket experiment: RH 200 rockets are basically meteorological rockets which attain an apogee in the range of 60 to 75 km. These rockets carry bundles of copper chaff of suitable dimensions. The chaff bundles are released close to the apogee altitude. The copper chaff drifts along with the ambient wind and is tracked by precision ground-based radars to give the position coordinates of the chaff as a function of time, from which the horizontal wind components are deduced. As the chaff descends with time, it gets diffused. As a result, the radar return signal becomes weak, rendering the position coordinate measurement ambiguous. Reliable track data can be obtained covering the altitude range 60 to 25 km. The horizontal wind component data are available at 1 km intervals. The errors involved in the wind measurement are given in Krishna Murthy *et al.*¹².

(ii) Balloonsonde: High-altitude balloonsondes reach an altitude of 30–35 km and are tracked by radars. From the radar track data, horizontal wind components are deduced at 1 km intervals. The error¹² in the deduced wind components is reported to be <2 m/s. Balloonsondes also carry temperature sensors to provide temperature data.

(iii) MST radar: The MST radar specifications are given by Rao *et al.*¹³. The radar operates at 53 MHz with an average power aperture product of $7 \times 10^8 \text{ Wm}^2$ and a range resolution of 150 m. The radar provides three-component wind data in the altitude range ~4 to 25 km and ~60 to 85 km. The radar can be operated in the temperature mode. From observations in this mode of operation^{14,15} temperatures can be deduced in the altitude range ~4 to 25 km, with a range resolution of 150 m.

Table 1. Details of experiments conducted in all equatorial wave campaigns

Campaign	Duration	Experiments	Location
First ¹²	23 May to 12 June 1984; Alternate days	RH 200 rockets and balloonsonde	Trivandrum, SHAR and Balasore
Second ³²	15 January to 28 February 1986; Daily	RH 200 rockets and balloonsonde	SHAR
Third ¹⁹	31 May to 12 July 1988; Daily	RH 200 rockets and balloonsonde	Trivandrum, Minicoy and Port Blair
Fourth ^{9,30}	September 1995 to August 1996; Daily	MST radar	Gadanki
Fifth ¹⁰	18 January to 5 March 1999; Daily	MST radar and Rayleigh lidar	Gadanki
Sixth ¹¹	21 February to 1 April 2000; Daily	MST radar and Rayleigh lidar; RH 200 rockets and balloonsonde	Gadanki; SHAR

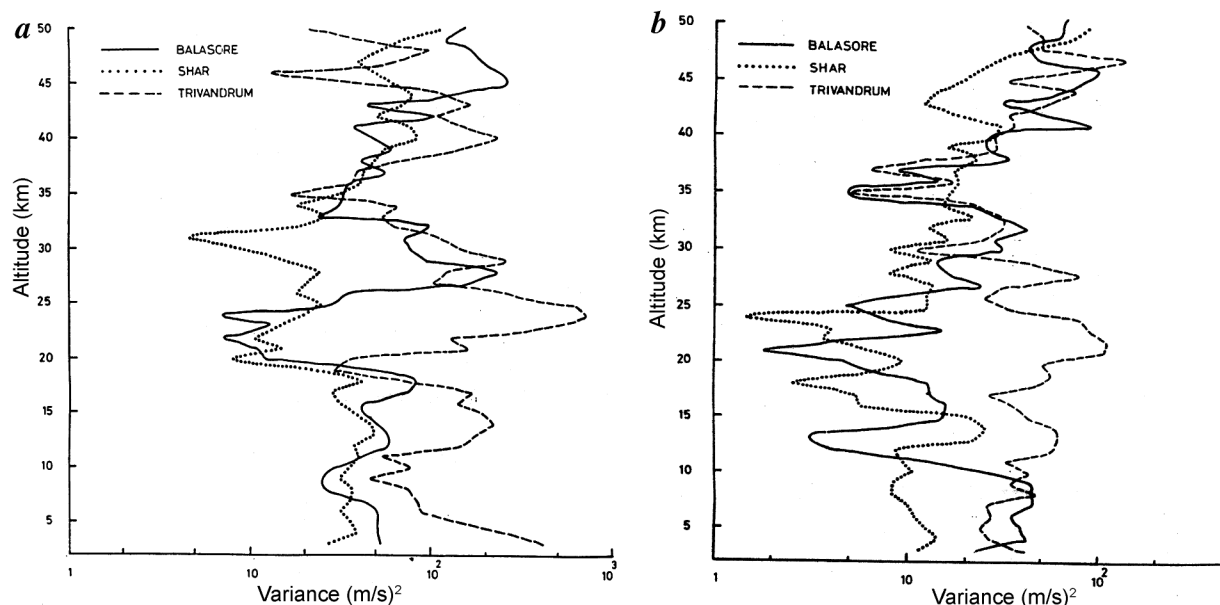


Figure 1. Variance of (a) zonal wind component and (b) meridional wind component as a function of altitude¹².

(iv) Rayleigh lidar: The Rayleigh lidar at Gadanki employs an Nd:YAG laser operated at its harmonic wavelength of 532 nm as the transmitter. The system details are given by Parameswaran *et al.*¹⁶. From the lidar data of backscatter, signal strength temperatures can be deduced with a resolution of 300 m in the altitude range ~27 to ~75 km. The errors involved in the temperature estimation are also dealt with in detail¹⁶.

Results of the campaigns

One of the objectives of the 1984 equatorial wave campaign was to study the latitudinal structure of the equatorial waves over the Indian subcontinent using wind data over Trivandrum (8.5°N, 77°E), SHAR (13.7°N, 80.2°E) and Balasore (21.5°N, 86.9°E). The wave characteristics at these stations revealed a couple of interesting aspects. An examination of the vertical structure of the zonal wind and meridional wind variances (a measure of strength of the temporal variations) shows that, in general, both Balasore and SHAR show smaller values compared to Trivandrum in many altitude regions as can be expected from the theoretical latitudinal variation of the equatorial wave amplitudes. But in certain altitude regions (troposphere and stratosphere), both zonal and meridional wind variances show greater values at Balasore compared to SHAR, as can be seen in Figures 1 *a* and *b*. In the upper stratosphere, zonal wind variance for Balasore is even larger than that for Trivandrum. This raises the possibility of penetration of extra tropical planetary wave activity into the tropical region.

Results from the 1984 campaign data showed a strong maximum in zonal wind variance in the altitude region 23 to

35 km over Trivandrum, SHAR and Balasore (Figure 1 *a*) and no phase propagation of waves of periodicities in the range 12–20 days was seen in this altitude region¹². Based on the observations in this campaign and using the ozone temporal fluctuations observed by Chandra¹⁷, Krishna Murthy *et al.*¹² had indicated the possibility of 25–35 km region acting as a source region for the generation of equatorial Kelvin waves with ozone fluctuations as the source, in addition to the tropical troposphere.

An interesting aspect of the vertical structure of the equatorial wave that has come out of the 1984, 1986 and 1988 campaigns, is the identification of a region of strong wave activity in the upper troposphere (between ~12 and ~16 km). This feature can be seen in Figures 1–3. This enhancement in wave activity is seen in both zonal and meridional components. It can be seen from Figures 2 *a* and *b* that contribution to this enhancement of wave activity is from the entire wave period range from ~42 to ~3 days. The second campaign data revealed presence of long period waves (>23 days) in the troposphere and is attributed to Rossby waves of extratropical origin penetrating to tropical latitudes.

The third campaign data revealed presence of Kelvin waves with periods in the range 12–16 days in the lower stratosphere, with a vertical wavelength of 10 km. Kelvin waves with shorter periods in the range 6–9.6 days are found to be present in the stratosphere and lower mesosphere, with a vertical wavelength of 10–15 km. RG waves with a period of 4–4.4 days and vertical wavelength of 10 km occurring below 20 km are also identified. Observations at Trivandrum (8.5°N, 77°E), Minicoy (8.3°N, 73°E) and Port Blair (11.7°N, 92.7°E) during the 1988 campaign period revealed that Rossby-gravity waves originated from the lower troposphere

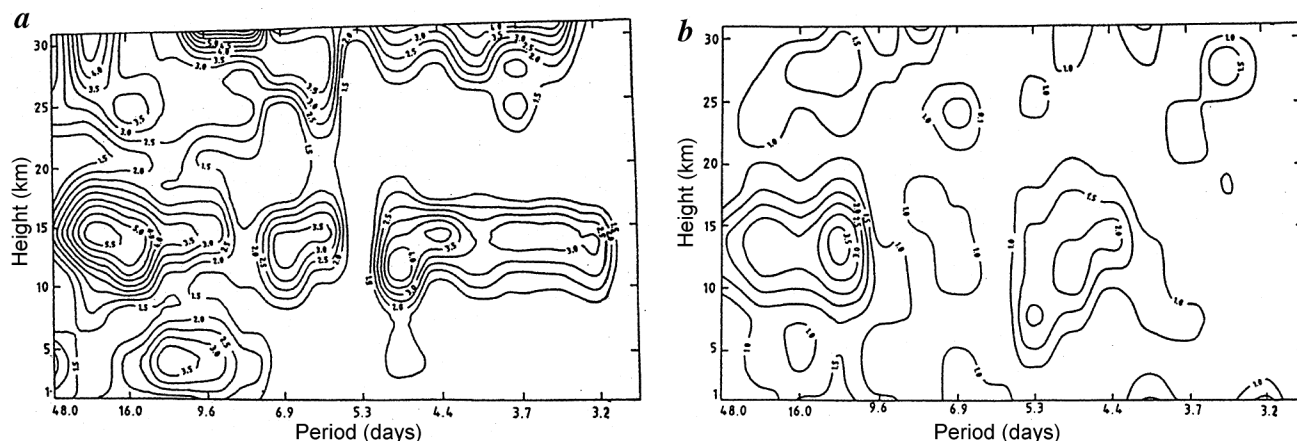


Figure 2. *a*, Amplitude spectrum of zonal wind oscillations in the 1–31 km height range at Trivandrum (8.5°N, 77°E); *b*, Same as (*a*) but for meridional wind oscillations⁹.

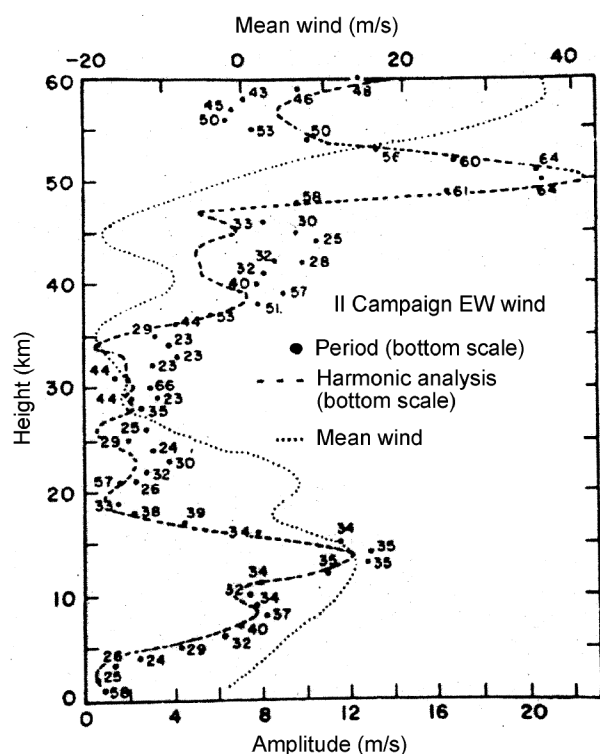


Figure 3. Variation of amplitude of long period (>23 days) waves with altitude. Dots and adjoining numbers represent amplitude and corresponding period as obtained by the ME method. Thin dotted curve (...) represents mean zonal wind for which the scale is provided at the top of the panel. Dashed curve (---) represents the amplitude obtained from harmonic analysis for a fundamental frequency of 45 days³².

(below ~8 km), as can be seen from the phase propagation characteristics over these stations (Figure 4 *a* and *b*). One interesting observation during the 1988 campaign was the modulation of fast Kelvin wave (6–9.6 days period) amplitude by the prevailing winds in the troposphere, stratosphere and mesosphere, as seen in Figure 5. It was reported that zonal winds reach their maximum amplitudes near the levels where

prevailing easterlies show a peak. Kelvin waves are eastward-propagating and their amplitudes are expected to grow exponentially with height as for any gravity wave. At the same time these waves are attenuated by radiative damping, which depends on their group velocity. The larger the group velocity, smaller the attenuation rate. The more the easterly background zonal flow, the more the group velocity and hence smaller the attenuation rate. Thus, whenever the easterly flow becomes stronger, the exponential growth of the Kelvin wave with height becomes stronger and the amplitude increases with altitude. Similarly, whenever the flow becomes more westerly, the exponential growth of the wave with height is inhibited because of the decreased group velocity and the consequent increase in radiative damping. Thus the Kelvin wave amplitude can be expected to be a maximum near the level of easterly maximum consistent with the observation.

In the 1984, 1986 and 1988 campaigns, the study of equatorial waves was based on wind data obtained using balloons in the troposphere and lower stratosphere, and RH-200 rockets in the stratosphere and lower mesosphere. Though radiosonde temperature measurements were made using high-altitude balloons during the 1988 campaign, data quality of temperatures (height resolution and coverage) was not satisfactory for a meaningful study of equatorial wave perturbations. The installation and operationalization of two important ground-based instruments, namely MST radar and Rayleigh lidar at Gadanki (13.5°N, 79.2°E) was a turning point in the investigation of equatorial waves over the Indian subcontinent. The MST radar has the capability of continuously (day and night) measuring tropospheric and lower stratospheric winds with 150 m height resolution and daytime mesospheric winds with 1.2/2.4 km height resolution (at discrete heights).

Taking advantage of the capability of the MST radar at Gadanki to provide three-component wind data, a campaign was conducted during September 1995 to August 1996 to deduce the wave momentum fluxes of equatorial waves⁹.

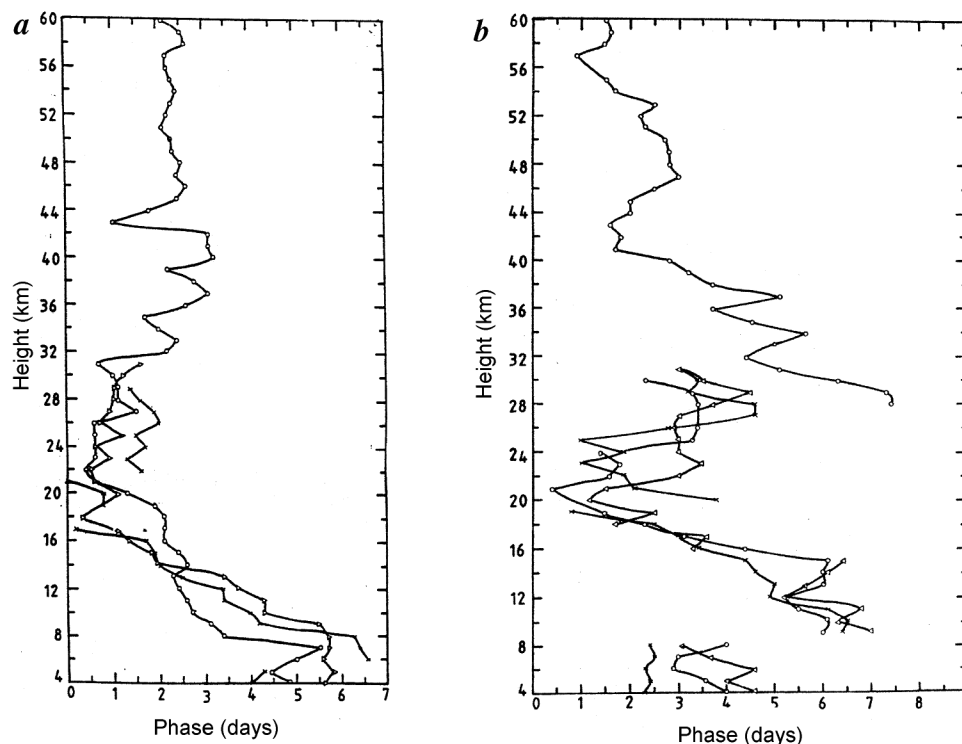


Figure 4. *a*, Phases (times of maximum eastward wind) of the 4–4.4 days zonal wind oscillations in height range 4–60 km at Trivandrum (lines joined by open circles), Minicoy (lines joined by triangles) and Port Blair (lines joined by crosses). *b*, Same as (*a*), but for meridional wind oscillations¹⁹.

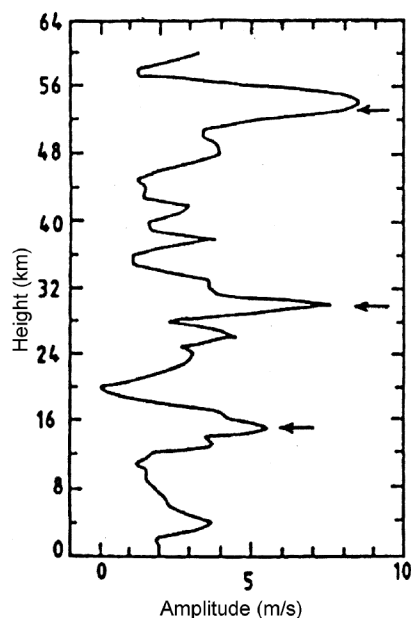


Figure 5. Amplitude of 6–9.6 days oscillations in zonal wind in the 1–60 km height range at Trivandrum. Heights of relative easterly (westward) peaks in mean zonal winds are indicated by arrows¹⁹.

This was for the first time that the equatorial wave momentum fluxes were estimated over the Indian zone. Using the three-component wind data, slow Kelvin waves with 12-day

period, fast Kelvin waves with 5.33-day period and RG waves with 3.43-day period were identified in the upper troposphere and lower stratosphere. The vertical flux of the zonal momentum was estimated for the four seasons, namely the two equinoxes and the two solstices, and was found to be a maximum in equinoxes for both Kelvin and RG waves. The flux values varied with season in the range 27 to $5.5 \times 10^{-3} \text{ m}^2 \text{ s}^{-2}$ for 12–8-day period Kelvin waves and in the range 6.7 to $2.1 \times 10^{-3} \text{ m}^2 \text{ s}^{-2}$ for 3–4-day period RG waves. These flux values are greater than those reported for slow Kelvin and RG waves using radiosonde data at Canton Island (2.8°S , 171.7°W)⁷.

The operation of MST radar in ‘temperature mode’ provides temperatures with good height resolution (150 m) in the troposphere and lower stratosphere^{14,15}. The Rayleigh lidar data could be used to derive temperatures with a 300 m resolution in the stratosphere and mesosphere¹⁶ on a regular basis. Thus from these two experiments, temperature profile can be obtained in the entire altitude range from 4 to 75 km. An experimental campaign had been conducted during January–March 1999 at Gadanki to delineate equatorial wave perturbations in temperature using MST radar and Rayleigh lidar. Significant equatorial wave perturbations in temperature with periods in the range 23.5–3.6 days in the 4–70 km altitude region were detected^{10,18}. Analysis of the temperature data obtained during the campaign shows that temperature fluctuations with periodicities in the 23.5–4.3

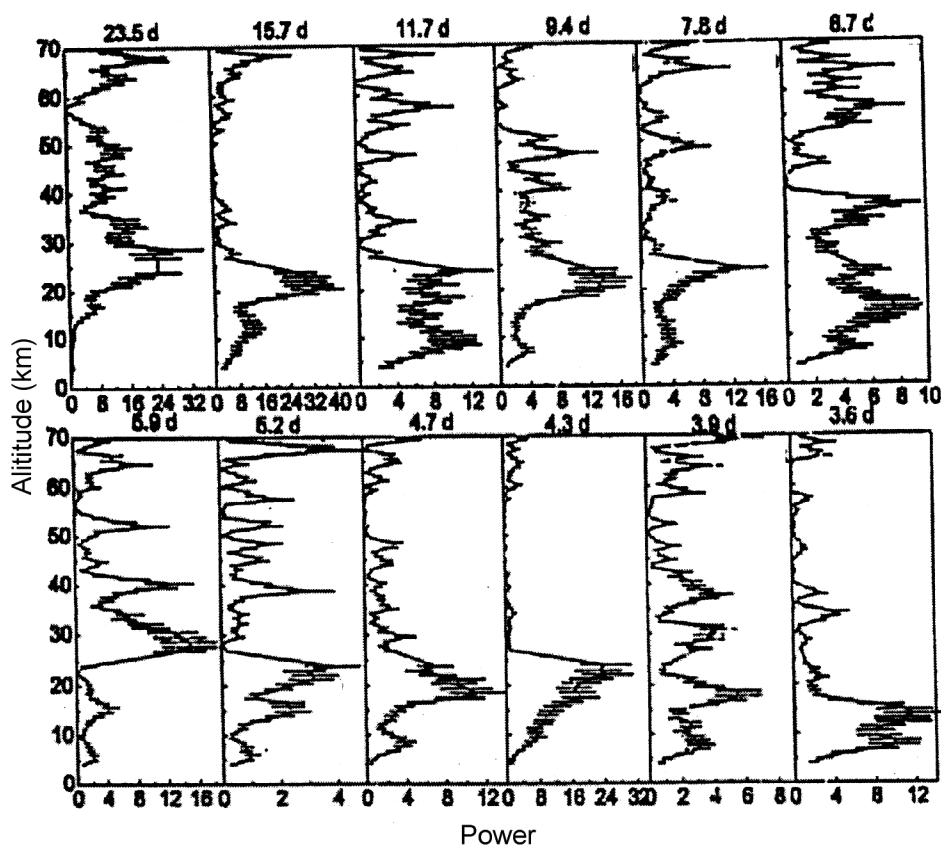


Figure 6. Altitude profiles of power of different periodicities in the range from 23.5 to 3.6 days. Horizontal bars represent the 90% confidence limits of estimated power. It may be noted that the X-axis scales are different in the different panels¹⁰.

days range attain, in general, their maximum in the lower stratosphere (20–25 km height) followed by a sharp decrease as shown in Figure 6. It can also be seen that the shorter periodicities of 3.9 and 3.6 days attain their maximum in the troposphere. Temperature perturbations in the 15.7–6.7 days in the troposphere and stratosphere are identified as due to Kelvin waves, with a vertical wavelength of ~ 10 km. In this band, only the shorter period Kelvin waves of 7.8 and 6.7 days penetrate into the mesosphere (Figure 7). This observation is consistent with the report by Dhaka *et al.*¹⁹ that Kelvin waves with period 6–9.6 days penetrate well into the mesosphere during summer season. In the troposphere and lower stratosphere, 15.7-day slow Kelvin wave has a zonal wavenumber 1, whereas the shorter period 9.4- and 7.8-day slow Kelvin waves have zonal wavenumber 2 and 6.7-day wave has a zonal wavenumber 3. As the background winds are found to be weak, the vertical flux of the zonal momentum could be estimated for the slow Kelvin waves in the period range 15.7 to 6.7 days. The reported values range from 2.8×10^{-3} to $0.18 \times 10^{-3} \text{ m}^2 \text{ s}^{-2}$, corresponding to the period range 15.7 to 6.7 days.

An important result of this campaign is the modulation of tropopause temperature and altitude by equatorial waves with periodicities of 15.7, 6.7 (which are due to slow Kelvin

waves) and 4.3 days, with a maximum amplitude of 4 K in tropopause temperature. The equatorial wave modulation of tropopause can affect transport of water vapour from the troposphere to stratosphere and stratosphere–troposphere exchange process²⁰. Waves with periods longer than about a week can be effective in dehydrating the tropical tropopause²⁰. In this context, the observed modulation of tropopause by equatorial waves assumes significance.

As mentioned earlier, an important parameter associated with the equatorial Kelvin and RG waves is the vertical flux of horizontal momentum, $u'w'$, where u' and w' are perturbations in zonal and vertical velocity respectively. This wave parameter is used in the QBO simulation in numerical models^{6,21}. However, QBO evolution is sensitive to any change in the wave flux (at ~ 17 km, the lower boundary of the models). Studies^{21–23} show that an increase in momentum fluxes leads to a decrease in the QBO period. The momentum fluxes of equatorial waves are usually estimated using the zonal wind and temperature data obtained from radiosonde measurements^{7,24}. There are only a few studies which deal with estimation of momentum fluxes associated with these waves in limited height ranges^{9,10,25,26}.

Recently, a coordinated experiment using ground-based MST radar and Rayleigh lidar, and meteorological rockets

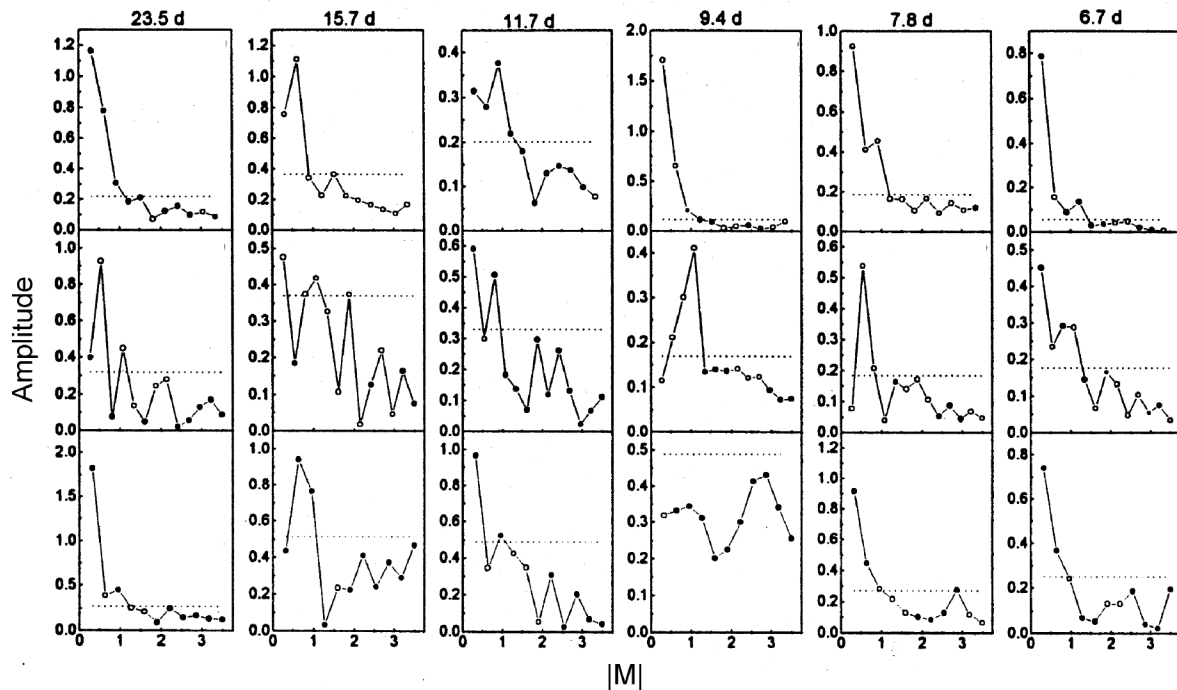


Figure 7. Altitude–vertical wavenumber (m) spectrum for periodicities in the range 23.5 to 6.7 days. Top panel, 4–25 km altitude range; middle panel, 27–50 km range and bottom panel, 50–70 km range. Open and filled circles represent negative and positive m respectively. Dotted horizontal line in each panel represents the corresponding noise ($+2\sigma$) level¹⁰.

and balloons, lasting 40 days, has been conducted to characterize equatorial waves and estimate the momentum fluxes associated with these waves by measuring temperatures and winds everyday in the troposphere, stratosphere and mesosphere up to about 80 km at two low-latitude stations, Gadanki (13.5°N, 79.2°E) and SHAR (13.7°N, 80.2°E). It is for the first time that such a coordinated experiment involving measurement of winds and temperatures in the entire region from troposphere to mesosphere to characterize equatorial waves has been carried out. During the campaign period, daily temperatures and winds in the troposphere, stratosphere and mesosphere were measured for 40 consecutive days using ground-based instruments, rockets and balloons. The campaign, which started on 21 February and ended on 1 April 2000, was conducted at two closely located low-latitude stations Gadanki and SHAR. The ground-based instruments, MST radar and Rayleigh Lidar are located at Gadanki. The high-altitude balloon and rocket measurements were carried out from SHAR. As far as the planetary scales of the equatorial waves are concerned, these two stations can be considered to be co-located.

Analysis of the 2000 campaign data showed that from 3 to 7 March 2000, a cooling anomaly occurred right from ~10 to 60 km, with the maximum anomaly magnitude of ~25 K in the 27–36 km height region in the stratosphere, as can be seen from Figure 8. There appears to be a zonal wind anomaly (winds becoming more easterly) below the stratopause at about the same time when anomalous cooling was observed. There is a long-period (15–20 days) perturbation

in the mesosphere, one cycle of which is discernible above ~55 km altitude. In the ~30–50 km region, much shorter period (~5 day) oscillation can be seen in zonal wind as well as in meridional wind with little phase propagation. This appears to originate after the occurrence of the large temperature and zonal wind anomalies in the first few days of the campaign period and lasts for about four cycles (Figure 8c). The maxima associated with each consecutive cycle of oscillation have hardly any downward descent, which indicates the evanescent nature of these waves. This tendency is clearer in the meridional wind fluctuations. It is likely that the temperature anomaly may play a role in the generation of these waves in the tropical stratosphere. The question of the source of the cooling anomaly and whether it is confined to the tropical region or is global, is not addressed here and is beyond the scope of the present article.

Figures 9a and b show vertical profiles of amplitudes and phases of 17-day period oscillations in temperature and zonal wind (over SHAR). It is seen that in the mesosphere, 17-day oscillations in both temperature and zonal winds show downward phase propagation with a shorter vertical wavelength λ_z (10–15 km) in the 47–57 km height region and a longer λ_z (~25 km) above. Theoretically expected value of λ_z for zonal wavenumber 1 – slow Kelvin wave, for zero background wind speed is ~10 km. The shorter λ_z may correspond to a slow Kelvin wave, which is likely to be dissipated completely below 60 km due to critical level interaction (in the prevailing westerly winds). The larger λ_z may correspond to a 16-day Rossby normal mode, as it can

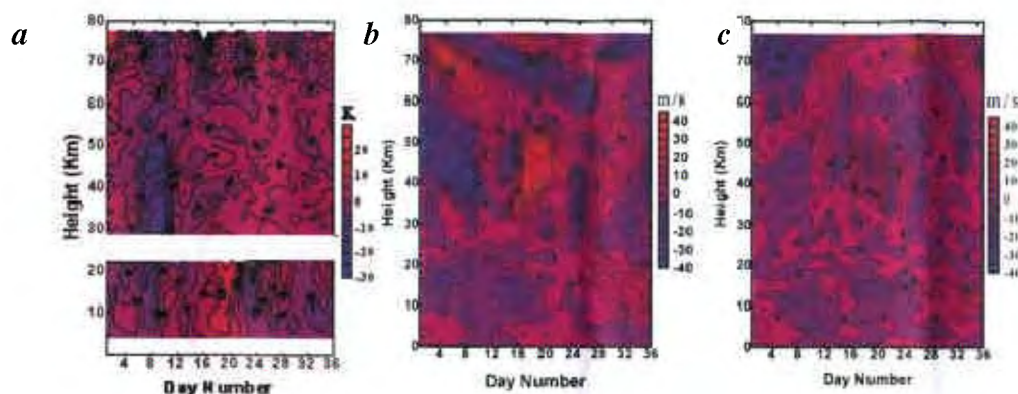


Figure 8. Height–time structure of fluctuations¹¹ in (a) temperature (K), (b) zonal winds (ms^{-1}) and (c) meridional winds (ms^{-1}) during 26 February–1 April 2000.

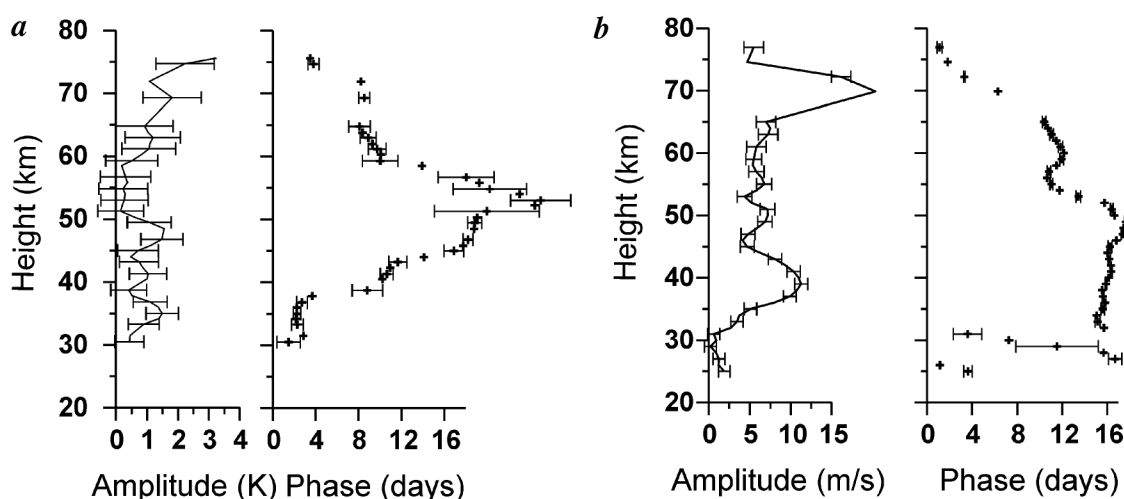


Figure 9. Height structure of amplitudes and phases of 17-day period Kelvin wave in (a) temperature and (b) zonal wind¹¹.

be expected to be significantly present during winter. In the stratosphere, downward phase propagation is not observed, except for zonal wind near 30 km.

Figures 10a and b shows vertical profiles of amplitudes and phases of 7.2-day period oscillation in temperature and zonal wind. It is seen that 7.2-day oscillation in temperature shows downward phase propagation in the height region of 30–50 km with a λ_z of ~ 15 km. The 7.2-day oscillation in zonal wind has downward phase propagation in the height region of 35–40 km, 50–80 km height region with a λ_z of ~ 15 km (theoretically expected value for zonal wavenumber 1 – fast Kelvin wave for zero background wind speed is ~ 20 km). The periods of oscillation, phase relationship between wind and temperature and observed λ_z along with smaller meridional wind fluctuations (from comparison of spectral powers) suggest that the 17-day (shorter λ_z of 10–15 km, below about 60 km) and the 7.2-day oscillations may be attributed to slow and fast Kelvin waves respectively.

An examination of the zonal winds in the 35–60 km during the first and second halves of the campaign period showed

that the zonal flow is under westerly acceleration in this height region (Figure 11a). However, it may be mentioned that stratospheric winds are likely to be affected by leakage of northern hemispheric planetary waves. In order to see whether the observed Kelvin waves are able to provide the necessary momentum to the mean flow to produce the observed acceleration, momentum fluxes (Figure 11b) were estimated from the cross spectra of temperature and zonal winds for slow and fast Kelvin waves. The mean flow acceleration produced by divergence of the momentum flux in the 35–60 km height region was compared with the zonal flow accelerations computed from the observed zonal winds (Figure 11c). It is seen that observed acceleration is much larger than that produced by the momentum flux divergence due to the Kelvin waves, indicating a deficit in the momentum budget in the evolution of the stratopause semi-annual oscillation (SSAO) in zonal wind. Contribution by the slow and fast Kelvin waves together is only $\sim 25\%$ of the observed acceleration. Notwithstanding the possibility of contamination by northern hemispheric planetary waves,

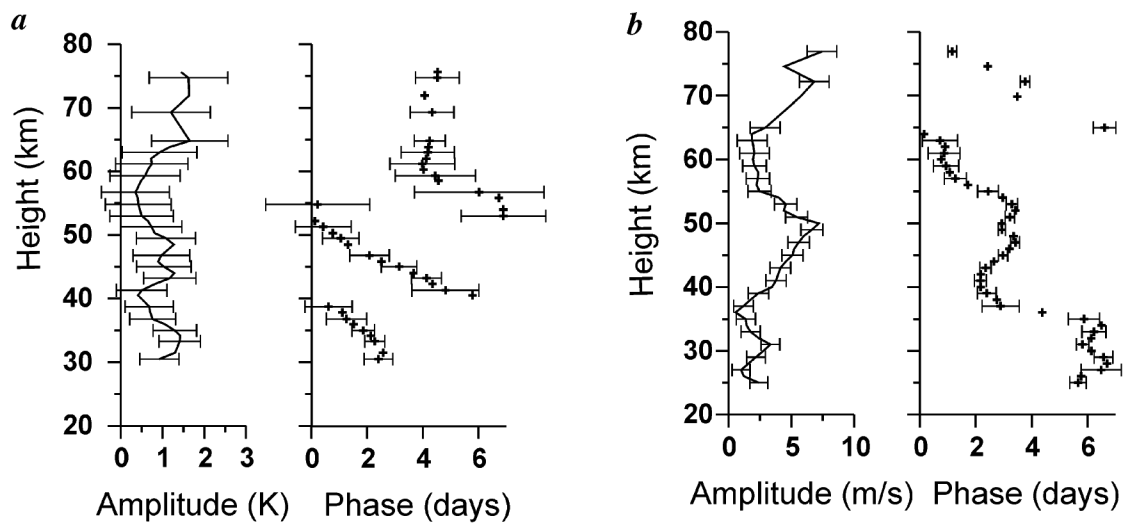


Figure 10. Height structure of amplitudes and phases of 7.2-day period Kelvin wave in (a) temperature and (b) zonal wind¹¹.

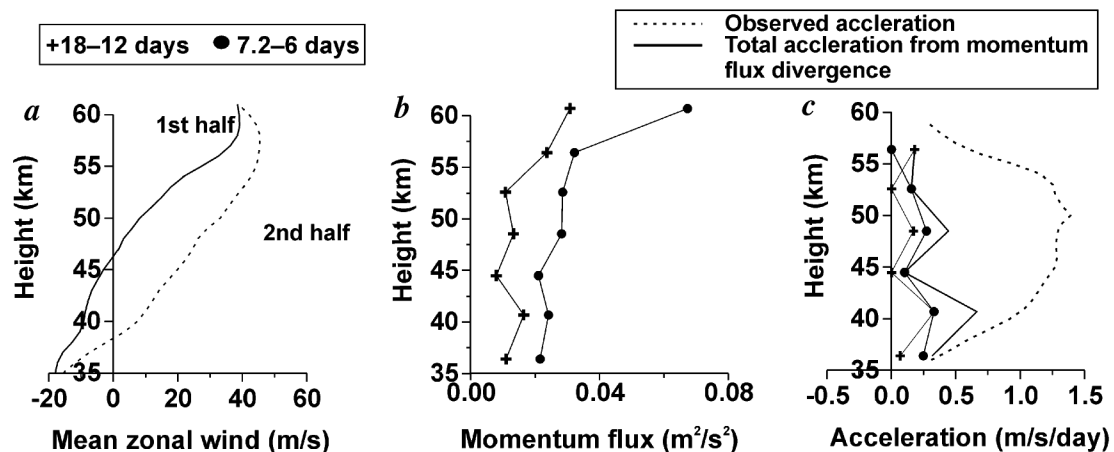


Figure 11. *a*, Time-mean zonal wind during first (thick line) and second half (dotted line) of the campaign period; *b*, Momentum flux of Kelvin waves; *c*, Observed acceleration and acceleration computed from momentum flux divergence of Kelvin waves¹¹.

the deficit could perhaps be accounted by other sources such as inertia gravity waves and gravity waves.

An important result of this campaign is the modulation of gravity wave activity by the equatorial waves in the tropical middle atmosphere²⁷. The observations reveal that the variability of the gravity wave activity in the tropical middle atmosphere is modulated by the wind oscillations due to the equatorial waves. This indicates that the variation of the gravity wave activity in the middle atmosphere can be attributed, at least partly, to the filtering process due to the interaction between the gravity waves and the background wind. The intrinsic phase speed of the gravity wave is the modulus of $(U-C)$ where U is the background mean wind speed and C is the phase speed of the wave. For a gravity wave spectrum with phase speeds distributed about zero, variation in U with a period T gives rise to gravity wave activity at period $T/2$. On the other hand, if the gravity wave

spectrum is asymmetric in phase speed, the gravity wave variance will occur at the same period²⁸ as U . Campaign observations showed that zonal wind in the lower stratosphere is strongly westward and the magnitude of this westward wind undergoes periodic fluctuations caused by gravity waves. The meridional wind in the stratosphere also undergoes significant fluctuations. The strength of gravity wave activity being a minimum when the westward and southward winds are maximum indicates that the gravity wave spectrum is asymmetric with a mean southwestward/westward phase speed.

Discussion

The main results of the equatorial wave studies described above can be summarized as follows.

1. Variance of zonal wind is greater at Trivandrum compared to SHAR and Balasore in the troposphere and lower stratosphere. In the upper stratosphere, the zonal wind variance is higher at Balasore, indicating the possibility of penetration of planetary wave disturbances of extra-tropical origin into the tropical middle atmosphere.
2. Kelvin wave amplitudes reach their maximum at altitudes near the level of easterly maximum.
3. Shorter period Kelvin waves (periods <9 days) can penetrate into the mesosphere whereas the longer period Kelvin waves are confined to the stratosphere and below. This finding has important implications to the generation of mesosphere SAO, as earlier observations revealed penetration of only much shorter period Kelvin waves (fast Kelvin waves) into the mesosphere⁴.
4. There is evidence for equatorial wave generation in the stratosphere.
5. There is evidence that RG waves originate below ~ 8 km.
6. The vertical wavelengths of the Kelvin waves in the period range 5–17 days are in the range of 10–15 km.
7. Tropopause altitude and temperature are modulated by equatorial waves in the period range ~ 15–4 days.
8. The mesospheric gravity wave activity is modulated by equatorial waves with periods of ~ 12 and ~ 4 days.
9. Vertical fluxes of horizontal momentum of Kelvin and RG waves are estimated.

The estimates of vertical flux of horizontal momentum (F) by different workers to date, including those from the campaigns presented above are summarized in Table 2. Before discussing the F values, a brief description of the methods of estimation of F is in order. Wallace and Kousky⁷ obtained F from the relation

$$F = (u'w')^* = ru^*w^*/2,$$

where u' and w' are the fluctuation amplitudes in zonal and vertical wind respectively; $*$ represents the average; r is the correlation coefficient between the zonal and vertical winds and u^* and w^* are the average amplitudes of zonal and vertical wind respectively. w^* is obtained from temperature fluctuations (T') using the standard thermodynamic relationship between the two as vertical wind data were not available. Sato and Dunkerton²⁴, and Holton²⁹ used essentially the same method, except that they used the quadrature spectra between u and T instead of the correlations. Sato and Dunkerton²⁴ found the errors in the estimated F as 0.5 to $0.8 \times 10^{-3} \text{ m}^2 \text{ s}^{-2}$. This error estimate can be taken to apply for the estimates of F by Holton²⁹, and Wallace and Kousky⁷. Krishna Murthy *et al.*¹⁰ estimated F from temperature fluctuations using the relations between T' and u' as also T' and w' . They reported the standard deviation in the F estimates to be $\pm 20\%$ of F . Sasi *et al.*⁹ and Sasi and Deepa³⁰ obtained the flux estimates directly from the quadrature spectra of u and w in the troposphere and lower stratosphere region. They reported an error in F of $\pm 1.2 \times$

$10^{-3} \text{ m}^2 \text{ s}^{-2}$. For estimates in the upper stratosphere and mesosphere, Sasi *et al.*¹¹, however, used quadrature spectra of u (from rocket sonde data) and T (from lidar data), as w is not available in this region.

It is seen that except in the estimates of F by Sasi *et al.*⁹ and Sasi and Deepa³⁰, in all other estimates the necessary vertical wind data were obtained from the temperature data. However, the procedure followed was quite similar in all the estimates and the reported errors (and standard deviations) in the F estimates are not high.

Though the F estimates available to date at different stations (Table 2) correspond to different years (and hence to different QBO cycles), useful inferences can be drawn from a comparison of these as discussed below.

Except the estimates at Gadanki, Balboa and Trinidad, all others belong to locations within 3° of the equator. The flux estimates at Nauru²⁹ corresponding to Kelvin waves in the period range 8–17 days and 4–6 days, are quite low compared to the others. However, the Nauru estimates correspond to the westerly phase of the QBO during which the eastward propagating Kelvin waves are expected to be weak. Other estimates which are higher than the Nauru estimates and for which the QBO phase is indicated, belong to the easterly phase of the QBO, during which the Kelvin waves are expected to be strong. The estimates at Singapore by Sato and Dunkerton²⁴, clearly demonstrate the dependence of the fluxes (of Kelvin waves) on the phase of the QBO, i.e. low fluxes during westerly phase of the QBO compared to the easterly phase. The Gadanki estimates (for Kelvin and RG waves) by Sasi and Deepa *et al.*³⁰ show a strong seasonal dependence with equinoctial values much higher compared to solstice values. This seasonal dependence has been attributed to the seasonal excursion of the Inter Tropical Convergence Zone (ITCZ). The ITCZ, which can be a source of equatorial waves, lies close to the equator during equinoxes and moves north and southwards during the solstices. Thus, during equinoxes, the ITCZ can be an effective source for the equatorial waves, which are confined to within 15° from the equator compared to solstices. It is reported in the literature that Kelvin wave activity reaches a maximum during solstice seasons and almost disappears during equinoxes³¹. This is in conflict with results from Gadanki³⁰, which showed an equinoctial maximum. It is well known that the seasonal excursion of the ITCZ is quite different at different longitude zones and is highest in the South Asian sector. The difference in seasonal dependence of Kelvin wave activity at Gadanki and other locations can be attributed to the differing seasonal excursions of ITCZ. It may be noted here that the seasonal dependence of Kelvin wave activity reported by Sasi and Deepa³⁰ corresponds to tropopause level and below, whereas that reported by earlier workers^{4,31} corresponds to altitudes $> 25 \text{ km}$ (middle stratosphere and above). The Kelvin wave activity strongly depends on background wind condition and altitude-dependent winds could affect seasonal dependence at different altitude ranges. This factor also needs to be taken into account while comparing

Table 2. Vertical fluxes of horizontal momentum of Kelvin and RG waves estimated by different authors

Authors	Location	Data	Season	Waves	Altitude region	Flux*	Comments
Wallace and Kousky ⁷	Balboa: 9°N, 80°W	Radiosonde	–	Slow Kelvin	Lower stratosphere	4	
	Trinidad, 11°N, 61°W					1	
Sato and Dunkerton ²⁴	Singapore: 1.4°N, 104°E	Radiosonde	–	20–5 d Kelvin	Lower stratosphere	2–9	QBO easterly shear
						2	QBO westerly shear
Sasi <i>et al.</i> ⁹	Gadanki: 13.5°N, 79.2°E	MST radar	Autumnal	12–8 d Kelvin	Tropopause region	16	
Sasi and Deepa ³⁰			Equinox	3–4 d RG		5.5	
			Vernal	12–8 d Kelvin		27	
			Equinox	3–4 d RG		6.7	
				12–8 d Kelvin		7.4	
			Winter	3–4 d RG		3.5	
				8–12 d Kelvin		5.5	
			Summer	3–4 d RG		2.1	
Holton <i>et al.</i> ²⁹	Nauru: 0.5°S, 166.9°E	Radiosonde	June–July	8–17 d Kelvin	18–25 km	0.1	QBO westerly shear
				4–6 Kelvin			
Krishna Murthy <i>et al.</i> ¹⁰	Gadanki: 13.5°N, 79.2°E	MST radar	January–February	15.7–6.7 d	4–25 km	2.8–0.18	QBO easterly shear
			1999	Kelvin			
Sasi <i>et al.</i> ¹¹	Gadanki: 13.5°N, 79.2°E	MST radar, Rocketsonde, lidar	February–March	18–12 d Kelvin	35–55 km	10	
			2000	7.2–6 d Kelvin		20–30	

*In units of $10^{-3} \text{ m}^2 \text{ s}^{-2}$.

the seasonal dependence of Kelvin wave activity at different altitude regions in addition to the longitudinal dependence.

The Gadanki estimates for Kelvin waves by Krishna Murthy *et al.*¹⁰ corresponding to the winter of 1999 are lower than those by Sasi and Deepa³⁰, corresponding to winter of 1996 and thus to a different QBO cycle. The flux contributions by equatorial waves could be different from cycle to cycle depending on the source and background atmospheric conditions²⁴. Sasi *et al.*¹¹ reported higher flux values during winter of 2000 at Gadanki. However, these values correspond to the altitude region 35–55 km, far removed from the troposphere source region, unlike all other estimates which correspond to lower altitude regions. In the altitude region 35–55 km, the waves can be expected to undergo growth in their strength and hence, the observed high flux values can be at least partly attributed to this factor. Further, these estimates are for a different QBO cycle (from other estimates). The flux values for RG waves are reported only by Wallace and Kousky⁷ and Sasi *et al.*¹¹. It is seen that the flux values are higher at Gadanki compared to those at Balboa and Trinidad, which are nearly at the same latitude but at a different longitude zone.

It is expected that the strength of equatorial waves decreases with latitude (within the region of 15° from the equator). However, the fluxes at Gadanki are, in general, higher than at the lower latitude locations (Table 2). Part of the reason could be that the estimates belong to different QBO cycles, as indicated above. The observed differences in the flux values between Gadanki and other locations could also be due to longitudinal differences in the strength of generation of the equatorial waves. This is an important factor

in the QBO study, as it is known that the latent heat releases in the troposphere, which is the prime source for the generation of the equatorial waves, can have large variation with longitude. Equatorial waves are known to possess horizontal wavelengths of the order of ten thousand kilometres and more, and thus are global in nature. The contribution of the latent heat releases at different longitudinal zones to driving the equatorial waves needs to be quantified. It is interesting to note here that Riggins *et al.*²⁵ attributed the observed differences in the Kelvin wave activity in the mesosphere at Jakarta (6.4°S, 107.6°E) and Christmas Island (1.9°N, 157.3°W) to differences in excitation source strength at the two locations situated at different longitudes.

Sasi *et al.*¹¹ and Sasi and Deepa³⁰ estimated the mean flow acceleration due to the vertical flux of the horizontal momentum of the observed Kelvin and RG waves and compared it with the observed mean flow acceleration. While the observed and estimated flow accelerations showed general agreement at tropospheric levels, the estimated accelerations fell short of the observed accelerations at stratospheric levels. The differences are reported to be more pronounced in solstices compared to equinoxes. At upper stratospheric and mesospheric levels, the fluxes due to equatorial waves account for only ~30% of the observed flow accelerations¹¹. This indicates that another source of momentum flux is necessary to account for the observed flow accelerations which result in the QBO and SAO. Gravity waves are the most likely source for this^{24,31}.

It is known that gravity waves play an important role in the generation of QBO, contributing to the required momentum flux²⁴. Gravity wave sources include troposphere convec-

tive activity, which has a strong seasonal and longitudinal dependence. The Gadanki results demonstrated the modulation of gravity waves in the middle atmosphere by equatorial waves. Thus, the effect of equatorial waves on the QBO and SAO in the middle atmosphere could also be indirect (in addition to the direct effect through contribution of momentum flux) through modulation of gravity wave activity, which contributes to the generation of QBO and SAO.

From the above discussion it is clear that a complete understanding of the generation of the equatorial middle atmospheric QBO and SAO requires quantification of equatorial wave and gravity wave momentum fluxes at locations in different longitude zones during a few cycles of QBO and SAO. This calls for a coordinated observational programme of middle atmospheric winds and temperature at locations in different longitude zones covering a few QBO (and SAO) cycles.

Conclusion

The main conclusions that emerge out of the results of the equatorial wave campaigns in the Indian zone are as follows:

- (i) The vertical wavelengths and periods of the observed Kelvin waves are in the ranges 10–15 km and 5–17 days respectively.
- (ii) Kelvin waves with periods shorter than ~9 days can penetrate into the mesosphere, whereas the longer period waves are confined to the stratosphere and below.
- (iii) There is evidence of penetration of extratropical planetary wave activity into the tropical middle atmosphere.
- (iv) The tropical tropopause is modulated by equatorial waves in the period range 4–15 days, with a maximum amplitude of 4 K in the tropopause temperature.
- (v) The gravity wave activity in the mesosphere is modulated by equatorial waves.
- (vi) The vertical flux of horizontal momentum of the equatorial waves reveals equinoctial maximum and solstitial minima in contrast to the behaviour at other longitude zones.
- (vii) A comparison of the vertical fluxes of horizontal momentum reported in the literature raises the question of substantial differences in the equatorial wave strength at different longitude zones.
- (viii) The vertical fluxes of the horizontal momentum of the equatorial waves are not adequate to account for the observed mean flow accelerations which result in the QBO and SAO.

1. Chang, C. P., Forcing of stratospheric Kelvin waves by tropospheric heat sources. *J. Atmos. Sci.*, 1976, **33**, 740–744.
2. Holton, J. R., Waves in the equatorial stratosphere generated by tropospheric heat sources. *J. Atmos. Sci.*, 1972, **29**, 368–375.
3. Holton, J. R., On the frequency distribution of atmospheric Kelvin waves. *J. Atmos. Sci.*, 1973, **30**, 499–501.

4. Hirota, I., Equatorial waves in the upper stratosphere and mesosphere in relation to the semi annual oscillation of the zonal wind. *J. Atmos. Sci.*, 1978, **35**, 714–722.
5. Reddy, C. A. and Vijayan, L., Reflection and attenuation of equatorial waves in the stratosphere and mesosphere. *Q. J. R. Meteorol. Soc.*, 1989, **115**, 1273–1299.
6. Holton, J. R. and Lindzen, R. S., An updated theory for the quasi-biennial cycle of the tropical stratosphere. *J. Atmos. Sci.*, 1972, **29**, 1076–1080.
7. Wallace, J. M. and Gousky, V. E., On the relation between Kelvin waves and the quasi-biennial oscillation. *J. Meteorol. Soc. Jpn.*, 1968, **46**, 496–502.
8. Maruyama, T., Equatorial wave intensity over the Indian Ocean during the years 1968–1972. *J. Meteorol. Soc. Jpn.*, 1979, **57**, 39–52.
9. Sasi, M. N., Lekshmi Vijayan, Deepa, V. and Krishna Murthy, B. V., Estimation of equatorial wave momentum fluxes using MST radar winds observed at Gadanki (13.5°N, 79.2°E). *J. Atmos. Sol-Terr. Phys.*, 1999, **61**, 377–384.
10. Krishna Murthy, B. V. *et al.*, A study of equatorial waves in temperature from 4 to 70 km using MST radar and lidar observations at Gadanki (13.5°N, 79.2°E). *Q. J. R. Meteorol. Soc.*, 2002, **128**, 819–838.
11. Sasi, M. N. *et al.*, A study of equatorial wave characteristics using rockets, balloons, lidar and radar. *Adv. Space. Res.*, 2003, **32**, 813–818.
12. Krishna Murthy, B. V., Indukumar, S., Reddi, C. R., Raghava Rao, R. and Rama, G. V., Results of equatorial wave campaign of IMAP in May–June 1984. *Indian J. Radio Space Phys.*, 1986, **15**, 125–138.
13. Rao, P. B., Jain, A. R., Kishore, P., Balamuralidhar, P., Damle, S. H. and Viswanathan, G., Indian MST radar Part I. System description and sample vector wind measurements in ST mode. *Radio Sci.*, 1995, **30**, 1125–1138.
14. Revathy, K., Prabhakaran Nair, S. R. and Krishna Murthy, B. V., Deduction of temperature profiles from MST radar observations of vertical wind. *Geophys. Res. Lett.*, 1996, **23**, 285–288.
15. Revathy, K., Prabhakaran Nair, S. R. and Krishna Murthy, B. V., Estimation of error in the determination of temperature using MST radar. *Indian J. Radio Space Phys.*, 1998, **27**, 241–243.
16. Parameswaran, K. *et al.*, Altitude profiles of temperature from 4 to 80 km over the tropics from MST radar and lidar. *J. Atmos. Sol-Terr. Phys.*, 2000, **62**, 1327–1337.
17. Chandra, S., Solar-induced oscillations in the stratosphere: A myth or reality? *J. Geophys. Res.*, 1985, **90**, 2331–2339.
18. Krishna Murthy, B. V. *et al.*, Preliminary results of equatorial wave experiment conducted from 18 January to 5 March 1999 with lidar at Gadanki. *Indian J. Radio Space Phys.*, 2000, **29**, 231–234.
19. Dhaka, S. K., Krishna Murthy, B. V., Nagpal, O. P., Raghava Rao, R., Sasi, M. N. and Sundaresan, S., A study of equatorial waves in the Indian zone. *J. Atmos. Terr. Phys.*, 1995, **57**, 1189–1202.
20. Holton, J. R., Haynes, P. H., McIntyre, M. E., Douglass, A. R., Good, R. B. and Pfister, L., Stratosphere–troposphere exchange. *Rev. Geophys.*, 1995, **33**, 403–439.
21. Geller, M. A., Shen, W., Zhang, M. and Tan, W. W., Calculations of the stratospheric quasi biennial oscillation for time-varying wave forcing. *J. Atmos. Sci.*, 1997, **54**, 883–894.
22. Plumb, R. A., The interaction of two internal waves with the mean flow: Implications for the theory of the quasi-biennial oscillation. *J. Atmos. Sci.*, 1977, **34**, 1847–1858.
23. Dunkerton, T. J., Wave transience in a compressible atmosphere. Part II: Transient equatorial waves in the quasi biennial oscillation. *J. Atmos. Sci.*, 1981, **38**, 298–307.
24. Sato, K. and Dunkerton, J., Estimates of momentum fluxes associated with equatorial Kelvin and gravity waves. *J. Geophys. Res.*, 1997, **102**, 26,247–26,261.
25. Riggan, D., Fritts, D. C., Tsuda, T., Nakamura, T. and Vincent, R. A., Radar observations of a 3-day Kelvin wave in the equatorial mesosphere. *J. Geophys. Res.*, 1997, **102**, 26,141–26,157.

-
26. Srikanth, R. and Ortland, D. A., Analysis of Kelvin waves in high resolution and microwave limb sounder stratosphere measurements using a constrained least squares method. *J. Geophys. Res.*, 1998, **103**, 23,131–23,151.
27. Parameswaran, K., Rajeev, K., Sasi, M. N., Geetha Ramkumar and Krishna Murthy, B. V., First observational evidence of the modulation of gravity wave activity in the low latitude middle atmosphere by equatorial waves. *Geophys. Res. Lett.*, 2002, **29**, 10.1029/2001GL013625.
28. Isler, J. R. and Fritts, D. C., Gravity wave variability and interaction with lower frequency motions in the mesosphere and lower thermosphere over Hawaii. *J. Atmos. Sci.*, 1996, **53**, 37–48.
29. Holton, J. R., Alexander, M. J. and Boehm, M. T., Evidence for short vertical wavelength Kelvin waves in the Department of Energy–atmospheric radiation measurement Nauru 99 radiosonde data. *J. Geophys. Res.*, 2001, **106**, 20,125–20,129.
30. Sasi, M. N. and Deepa, V., Seasonal variation of equatorial wave momentum fluxes at Gadanki (13.5°N, 79.2°E). *Ann. Geophys.*, 2001, **19**, 985–990.
31. Canziani, P. O., Holton, J. R., Fishbein, E. and Froidevaux, L., Equatorial wave variability during 1992 and 1993. *J. Geophys. Res.*, 1995, **100**, 5193–5202.
32. Raghava Rao, R., Suhasini, R., Sridharan, R., Krishna Murthy, B. V. and Nagpal, O. P., Vertical structure and characteristics of 23–60 day (zonal) oscillations over the tropical latitudes during the winter months of 1986 – Results of equatorial wave campaign-II. *Proc. Indian Acad. Sci. (Earth Planet. Sci.)*, 1990, **99**, 413–423.
-

Received 21 October 2004; revised accepted 9 May 2005